Sixth International Symposium on Coastal Sediment Processes - Coastal Sediments '07. Coasts, Oceans, Ports and Rivers Institute (COPRI) of the American Society of Civil Engineers, May 13-17, New Orleans, Louisiana. Volume 2, pp. 1075-1088.

RECONSTRUCTING TSUNAMI RUN-UP FROM SEDIMENTARY CHARACTERISTICS – A SIMPLE MATHEMATICAL MODEL

Richard L. Soulsby[1], David E. Smith[2], Alan Ruffman[3]

1. HR Wallingford Ltd, Howbery Park, Wallingford, Oxfordshire OX10 8BA, UK (for correspondence) and Dept of Engineering Science, University of Oxford, UK. r.soulsby@hrwallingford.co.uk
2. School of Geography, Oxford University Centre for the Environment, South Parks Rd, Oxford OX1 3QY, UK. david.smith@ouce.ox.ac.uk.
3. Geomarine Associates Ltd, PO Box 41, Stn.M, Halifax, Nova Scotia B3J 2LJ, Canada. aruffman@dal.ca

Abstract: Tsunamis frequently leave a characteristic sediment deposit on the inundated land surface, which can be interpreted to deduce some of the features of the original tsunami wave. A simple trajectory-based theory of the tsunami hydrodynamics and sediment dynamics is presented here, yielding expressions for the landward variations in thickness and sediment composition of the deposit. Each grainsize contribution to the deposit thins linearly landwards, with the sediment run-up limit increasing with decreasing grainsize. The expressions can be fitted to observed sedimentary characteristics to deduce the run-up height and distance of the water. Example applications of the theory are given for the 1929 "Grand Banks" Tsunami, and the Holocene Storegga Slide Tsunami. Reconstruction of palaeo-tsunamis can help with assessments of present day risks from tsunamis.

INTRODUCTION

Evidence can be found at many locations around the world of thin layers of sand that are attributed to deposition by tsunamis. These have been observed after modern tsunamis, and can also be found in the recent geological record as evidence of tsunami inundation in the past. They typically run some 100s of metres inland of the (historic) shoreline and are up to some 10s of centimetres thick. Typically, they comprise a fine to medium sand with only small amounts of fine silt and clay, in a layer that thins from the shoreline landwards (e.g. Smith *et al.* 2004; Matsutomi *et al.* 2001; Dawson and Shi 2000; Moore 2001). Detailed grainsize analysis of vertically subdivided borehole samples generally reveals a pattern of landward fining, with upward fining in one or more sequences (Smith *et al.* 2004). Observations following modern tsunamis have shown that the height and landward extent of inundation by the water extend further than the limit of the sediment deposits (Tuttle et *al.* 2004) .

The aim of the present paper is to devise a simple mathematical model that contains the main physical (hydrodynamic and sediment dynamic) processes needed to predict the behaviour described above. The derived equations describing the characteristics of the sediment deposits are expressed in terms of the main descriptors of the coastal profile, the sediments and the tsunami hydrodynamics. Previous research workers have devised physics-based methods to re-construct the maximum inundation depths (Smith *et al.*, in press), maximum velocities (Jaffe and Gelfenbaum, in press), and characteristic velocities and depths together (Moore *et al.*, in press). The present approach extends these and other analyses (e.g. Matsutomi *et al.* 2001; Dawson and Shi 2000) by including a fuller description of the tsunami dynamics, while remaining mathematically tractable. A major motivation for this work is to facilitate re-construction of palaeo-tsunamis to assess the present-day risk of tsunamis at coastal sites, using the rationale outlined by Jaffe and Gelfenbaum (2002).

DERIVATION OF THEORY

Conceptual model

The scenario considered is sketched in Figure 1, which also shows the notation used. In order to keep the model mathematically tractable, a number of simplifying assumptions have been made. Everything is taken to be constant in the along-shore direction (1D assumption), and only the inundation flow onto and off the dry land is considered. The land surface is assumed to be plain and non-erodible, with a slope of 1:m. If R_z is the maximum run-up height of the water, then the maximum horizontal run-up distance is $R_w = mR_z$ from the still-water shoreline (SWL).

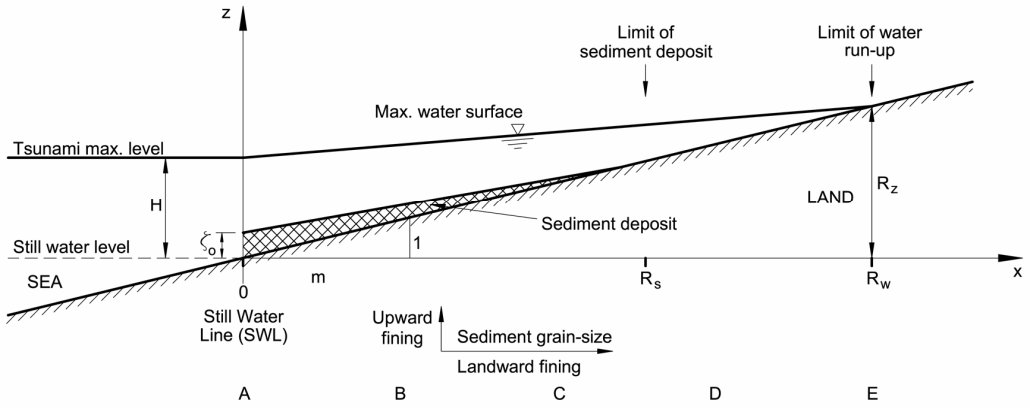

Fig. 1. Schematic of cross-section through land surface, with tsunami inundation and deposits. Snapshot at time $t = \gamma T$. ζ_0 is deposit thickness at SWL.

Considering first the *hydrodynamics* of the tsunami wave, the maximum depth of inundation is assumed to decrease linearly with distance x from the SWL, from a depth H at $x = 0$ to zero at the maximum run-up point (Figure 1). The water depth $h(0,t)$ at the SWL (Point A in Figure 1) is assumed to increase with time linearly to H during the uprush ($0 < t < \gamma T$), then decrease linearly with time during the backwash ($\gamma T < t < T$), where T is the total time that the SWL is inundated (Figure 2a).

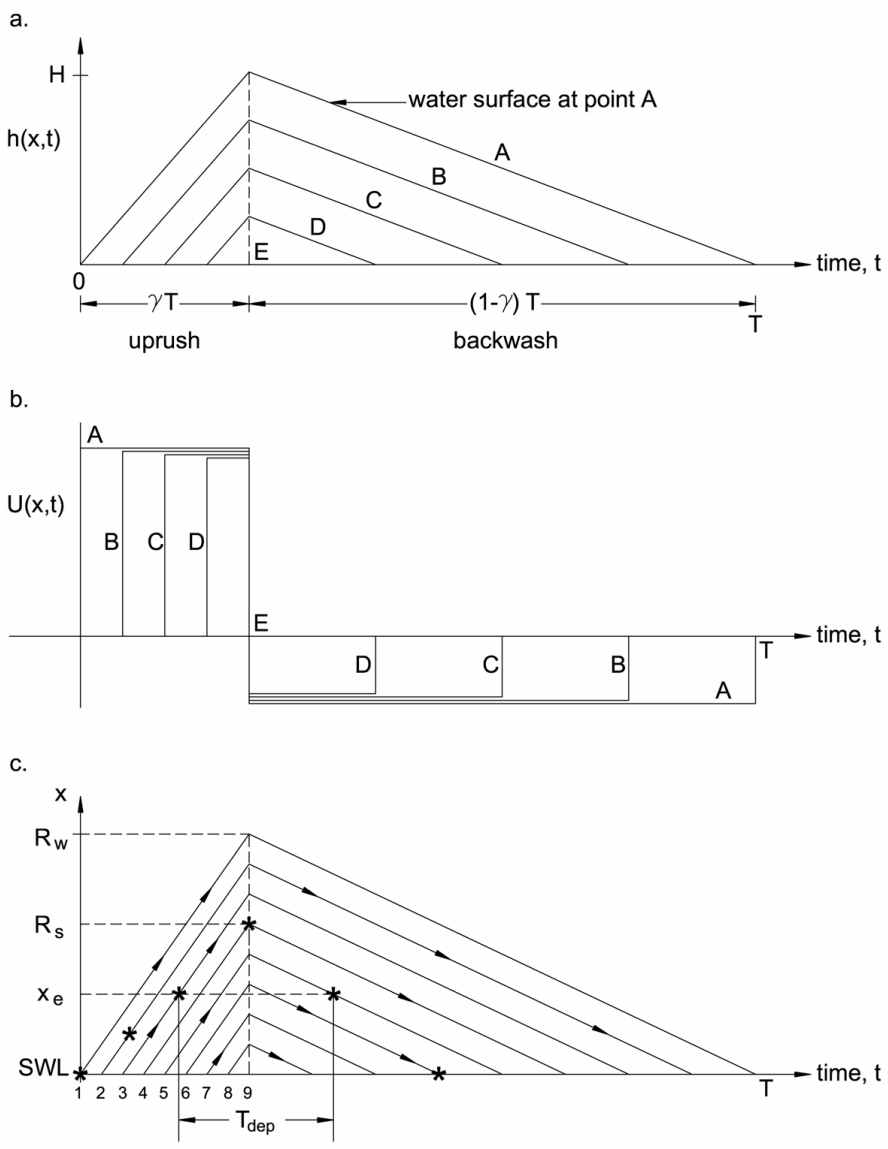

Fig. 2. Idealised tsunami characteristics for modelling purposes. (a) Depth variation with time at points A – E on Fig. 1. (b) Velocity variation with time at points A – E on Fig. 1. (c) Trajectories of water particles as distance (x) inland of SWL versus time for 9 different times of crossing the SWL. R_w and R_s are the horizontal run-up limits of water and sediment respectively, * marks points at which sediment deposition ceases for each trajectory, and T_{dep} is the duration over which sediment is deposited at example point x_e.

The time-variation of the water-level $h(x,t)$ at points between A and E also increases and decreases linearly with time, and the inundation durations decrease linearly with x from T at Point A to zero at Point E (Figure 2a). The time-lag between the time of maximum inundation at Point A and at the successive Points B to E is ignored, i.e. maximum water-level occurs everywhere at time $t = \gamma T$. Depth-averaged water

velocities $U(x,t)$ are derived from the prescribed depths via the continuity equation (Figure 2b).

Next, considering the *sediment dynamics*, the wave is assumed to be heavily charged with suspended sediment eroded from the sea bed when it arrives at the SWL (Point A). The concentration (dry mass per unit volume) here is taken as constant (C_o) through the depth due to intense turbulent mixing, and constant in time over the uprush period $t = 0$ to γT during which sediment is advected onshore. Initially, the sediment is treated as having a single grain-size with settling velocity w_s. This is easily extended later to multiple grain-sizes. Judging from the observed thicknesses of deposits, the concentrations of suspended sediment must be very large (some 10s or 100s of kg/m^3), so that the downward settling flux $w_s C_o$ of sediment greatly outweighs the re-erosion flux. Accordingly, for the purpose of this simple model, the re-erosion flux is neglected. The settling is treated as if the sediment was in a moving settling column, i.e. the settling flux is given by a constant value of $w_s C_o$ until all the sediment in that water column has been deposited. This ignores the re-distribution of sediment vertically by turbulence. The thickness of the sediment deposit is assumed to be much thinner than the inundation depth, so that the changing bed elevation during the inundation does not significantly affect the hydrodynamics.

Mathematical model

A brief summary of the derivation of the model is presented here. The full mathematical derivation is available from the first author on request. Following Borthwick *et al.* (2005), the continuity equation is expressed in the form:

$$\frac{\partial h}{\partial t} + \frac{\partial q}{\partial x} = 0 \tag{1}$$

where the volumetric flux q of water (per unit shore-wise width) is given by: $q = Uh$ and q, U and h are all functions of x and t. From the prescribed form of depth time-series shown in Figure 2a, it can be seen that $\partial h/\partial t$ is a positive constant during the period $t = 0$ to γT, and a negative constant during the period $t = \gamma T$ to T. Solution of Eq. 1 during the uprush phase leads to a velocity that is constant in time and space (Figure 2b):

$$U_{up} = \frac{R_w}{\gamma T} \tag{2}$$

Likewise, during the backwash phase the velocity is also constant:

$$U_{back} = -\frac{R_w}{(1-\gamma)T} \tag{3}$$

Consider the nine trajectories of water particles shown in Figure 2c. Because of the assumptions made, the water depth remains constant along any trajectory. Thus trajectory 1 is the locus of the wetting and drying line, has depth $h(x,t) = 0$, and reaches inland to the run-up limit R_w. Trajectory 3 starts at time $t = \gamma T/4$, has depth $h(x,t) = H/4$, and reaches inland to $x = (3/4)\, R_w$. Trajectories 5 and 7 have depths $H/2$ and $3H/4$, and reach inland distances $x = R_w/2$ and $R_w/4$ respectively. Trajectory 9

has a depth H, but because it starts (and finishes) at time $t = \gamma T$, it does not travel inland at all.

Applying the assumption that the sediment settles as it would in a settling column, the time taken for all the initially-suspended sediment to settle onto the bed, with settling velocity w_s, is h/w_s. Thus trajectories with greater depths will deposit sediment for longer times. Conversely, as seen above, these trajectories are also the ones with the shorter durations (from crossing the SWL on the uprush to re-crossing it on the backwash), and have the shorter penetrations inland. In Figure 2c, the point at which all the suspended sediment has been deposited is marked * on each trajectory. Trajectory 1 has zero depth, so all sediment is dropped immediately. Trajectories 2 and 3 have progressively greater depths, and complete the deposition at progressively later times and further distances inland. Trajectory 4 just completes its deposition at time $t = \gamma T$, when its distance inland is a maximum and it is about to return with the backwash. This distance, denoted R_s, is the maximum run-up distance for sediment deposition. Trajectories 5 and 6 are sufficiently deep that sediment is not only deposited during the uprush, but also through part of the backwash. Trajectory 6 just completes its deposition by the time it returns to the SWL. Trajectories 7 and 8 deposit sediment through their entire uprush and backwash journeys and carry some sediment back out to sea. Trajectory 9 does not carry sediment onto the land.

Now consider an arbitrary fixed point x_e on the land surface (see Figure 2c). No sediment arrives at point $x = x_e$ until trajectory 3 arrives. All the subsequent trajectories deposit sediment at $x = x_e$ until trajectory 5, which completes deposition on the backwash at $x = x_e$. Trajectory 6 deposits sediment briefly at $x = x_e$, but trajectories 7 and 8 do not even reach $x = x_e$. The time during which sediment is deposited T_{dep} extends from the time trajectory 3 reaches x_e on the uprush to the time trajectory 5 reaches x_e on the backwash. Moreover, with the settling column assumption, the rate of deposition during this time is constant = $w_s C_0$, so that the total mass of sediment deposited at point $x = x_e$ throughout the inundation is $w_s C_0 T_{dep}$. This applies to all points x_e between $x = 0$ and R_s, with T_{dep} decreasing landwards.

The run-up distance for sediment, R_s, can be related to the run-up distance for water, R_w (Figure 1), as follows. Suppose that trajectory i (which crosses the SWL at time $t = t_i$) is the one that just completes deposition at the time of velocity reversal, $t = \gamma T$ (marked as trajectory 4 on Figure 2c). Because depth at the SWL ($x = 0$) increases linearly with time during the uprush, the depth of this trajectory is:

$$h_i = \frac{t_i}{\gamma T} \cdot H \tag{4}$$

The time during which the trajectory is moving landwards is $(\gamma T - t_i)$, and this is equal to the time taken to deposit all the sediment, h_i/w_s. Thus:

$$\gamma T - t_i = \frac{h_i}{w_s} \tag{5}$$

Since the velocity on the uprush is given by Eq 2, the maximum distance R_s inland that sediment is deposited is (making use of Eqs. 2, 4 and 5):

$$\begin{aligned} R_s &= U_{up}\left(\gamma T - t_i\right) \\ &= R_w \cdot \frac{1}{w_s \gamma T / H + 1} \end{aligned} \tag{6}$$

For convenience, write $\alpha = \frac{w_s T}{H}$. Then the run-up of sediment R_s is related to the run-up of water R_w by the relationship

$$R_s = \frac{R_w}{1+\alpha\gamma} \tag{7}$$

Now calculate the thickness, ζ_o, of sediment deposited at the SWL ($x = 0$). Consulting Figure 2c, sediment starts to be deposited at $x = 0$ by trajectory 1, and finishes depositing at the end of trajectory 6. Denote this final depositing trajectory as trajectory j, which crosses the SWL on the uprush at time $t = t_j$, and reaches the SWL again on the backwash at time $t = t_k$. The trajectory has a depth h_j, and hence deposits all its sediment in a time h_j/w_s which is equal to the duration ($t_k - t_j$) of the trajectory. Thus:

$$t_k - t_j = \frac{h_j}{w_s} \tag{8}$$

The depth is given by (see Eq 4)

$$h_j = \frac{t_j}{\gamma T} \cdot H \tag{9}$$

and t_k is related to t_j by the respective velocities of uprush and backwash. The distance travelled inland is equal to U_{up} ($\gamma T - t_j$) on the uprush, and distance travelled back to the SWL is equal to $|U_{back}|$ ($t_k - \gamma T$) on the backwash. Equating these, and making use of Eqs 2, 3, 8 and 9 leads to:

$$\begin{aligned} t_k &= T - \frac{(1-\gamma)}{\gamma} \cdot \frac{\alpha\gamma T}{1+\alpha} \\ &= T \cdot \left[\frac{1+\alpha\gamma}{1+\alpha}\right] \end{aligned} \tag{10}$$

This gives the time $T_{dep,0} = t_k$ during which sediment is deposited at $x = 0$. Since sediment is deposited continuously at the rate $C_0 w_s$ through time $T_{dep,0}$, the mass deposited per unit area of bed at $x = 0$ is $C_0 w_s T_{dep,0}$. If the (dry) bulk density of the deposited sediment is ρ_B, where a typical value is $\rho_B = 1600\text{kg/m}^3$, the thickness deposited, ζ_o, is (using Eq. 10)

$$\zeta_o = \frac{C_0 w_s T}{\rho_B (1+\alpha)}(1+\alpha\gamma) \tag{11}$$

and, since $w_s T = \alpha H$,

$$\zeta_o = \frac{\alpha(1+\alpha\gamma)}{1+\alpha} \cdot \left(\frac{C_0}{\rho_B}\right) \cdot H \tag{12}$$

A full mathematical analysis following the same principles outlined above, and extended to all points inland, gives the distribution of the thickness $\zeta(x)$ deposited decreasing with distance x inland of the SWL according to the linear relationship:

$$\zeta(x) = \zeta_0\left(1 - \frac{x}{R_s}\right) \quad \text{for } x \le R_s, \text{ and 0 for } x > R_s \tag{13}$$

where ζ_o is given by Eq (12), R_s is given by Eq (7), and $\alpha = \frac{w_s T}{H}$.

Interpretation

The analysis given above enables the distribution of the thickness of sediment deposit, $\zeta(x)$, left by a single tsunami wave to be predicted for a wave of maximum height H at the SWL, with a period T from the time of first wetting to final drying at the SWL, in which the uprush occurs during a fraction γ of that period.

The deposit has a maximum thickness ζ_o occurring at the SWL, given by Eq 12. For a very fine-grained sediment (clay or fine silt), w_s is very small so α is very small and ζ_o tends to zero. Thus very fine sediments are hardly deposited at all, because they stay in suspension throughout the inundation. For coarser-grained sediment (coarse silt or sand), w_s is larger so α is larger, and the thickness ζ_o increases with grain-size (for a given concentration C_0). The thickness of the deposit is proportional to the concentration of suspended sediment just offshore of the SWL, and increases with the proportion γ of time occupied by the uprush. For very coarse-grained sediment, α is large and ζ_o tends to a value of $\alpha\gamma C_0 H/\rho_B = w_s(\gamma T)(C_0/\rho_B)$; in other words, all the suspended sediment is deposited during the uprush (γT) near the SWL.

The thickness of deposit tapers inland linearly with distance (x) from the SWL, as given by Eq 13, up to the sediment run-up distance R_s. Beyond this, no sediment is deposited, even though the water runs up further, to a distance R_w. R_s is smaller than R_w by a factor $(1+ \alpha\gamma)$ as given by Eq 7. Thus, for a given γ, the larger that α is (coarse sediments), the shorter the sediment run-up. Very fine sediments will extend almost to the limit of water run-up, but gravel and coarse sand will be deposited closer to the SWL. For a given sediment size, the run-up distance R_s decreases as the proportion γ of time occupied by the uprush increases.

Mixed sediments

If interactions between different grain-sizes of a mixed sediment are ignored, Eqs 13, 7 and 12 can be applied separately to different grain-size fractions. Each fraction (subscript n) will have a characteristic settling velocity w_{sn} and characteristic value of α_n (for a tsunami of given H and T), and will have a concentration C_{on} just offshore of the SWL.

As an illustration, consider the case of a tsunami with a wave height of H = 5m, period T = 10 minutes, and uprush occupying 2.5 minutes (γ = 0.25), striking a coast that has a slope of 1:m = 1:30. The wave has entrained sediment characterised as follows into three grain-size fractions, each having a concentration of 20kg/m^3 (total concentration = 60kg/m^3). The fractions are, using subscripts n = 1, 2, 3:

Finest 1/3, represented by d_{16} = 0.1mm, with w_{s1} = 0.006m/s and C_{01} = 20kg/m^3
Middle 1/3, represented by d_{50} = 0.2mm, with w_{s2} = 0.02m/s and C_{02} = 20kg/m^3
Coarsest 1/3, represented by d_{84} = 0.4mm, with w_{s3} = 0.053m/s and C_{03} = 20kg/m^3

Suppose that the run-up height of the water is R_z = 8m, so that the run-up distance is $R_w = 8 \times 30 = 240$m. Using Eqs (12) and (7) for each fraction:

Fine sediment: $\alpha_1 = \dfrac{0.006 \times 10 \times 60}{5} = 0.72,\ \zeta_{01} = 0.031m,\ R_{s1} = 203m$

Medium sediment: $\alpha_2 = \dfrac{0.02 \times 10 \times 60}{5} = 2.4,\ \zeta_{02} = 0.071m,\ R_{s2} = 150m$

Coarse sediment: $\alpha_3 = \dfrac{0.053 \times 10 \times 60}{5} = 6.4,\ \zeta_{03} = 0.140m,\ R_{s3} = 93m$

When the three fractions are added together, it is seen that they form a landward-fining sequence. In addition, since the coarse fraction is deposited first, and the fine fraction last, at any point, they will form an upward fining sequence. The composition of each upward fining sequence could be calculated by an extension of the mathematical analysis that would give the time-sequence of deposition for each fraction at each point.

APPLICATION 1: THE 1929 "GRAND BANKS" TSUNAMI

On November 18th, 1929, a magnitude M_s = 7.2 earthquake on the Grand Banks south of Newfoundland triggered an offshore landslide that developed into a turbidity current moving down the Continental Slope and out onto the Abyssal Plain, cutting twelve trans-Atlantic telegraph cables. The resulting tsunami was observed from Newfoundland to the Caribbean, being felt most strongly on the south coast of the Burin Peninsula, southern Newfoundland. The tsunami run-up rose to 13m above the normal tide level in St. Lawrence, and to about 10m at Taylor's Bay, both south-facing bays. Widespread devastation took place on the Burin Peninsula and 28 persons lost their lives (Tuttle *et al.* 2004, Ruffman and Hann 2006).

The site from which the samples analysed in this paper were obtained is at Taylor's Bay, on the south side of the Burin Peninsula (Figure 3). At Taylor's Bay, a sand and gravel barrier circa 200m long encloses a small lagoon, landward of which an area of low-lying, largely peat-covered land, up to 20m above local datum, widens to nearly 1km behind the lagoon, then progressively narrows for circa 500m inland. The site is of particular interest for studying the effects of the tsunami because there are records of the arrival of the waves across the barrier and into the low-lying area and of the destruction caused, so that there is anecdotal evidence of the anatomy of the event (Tuttle *et al.* 2004). However, the particular value of the site lies in the extensive deposit of sand which was deposited by the tsunami and which is found a few cm

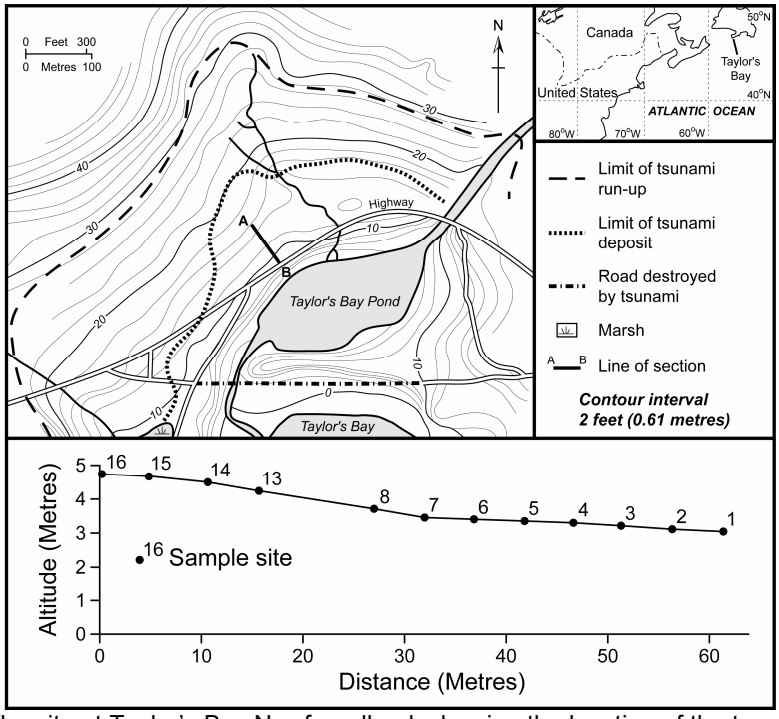

Fig. 3. The site at Taylor's Bay Newfoundland, showing the location of the transect from which samples were taken, together with the possible limits of tsunami run-up and deposit. Based partly on Tuttle *et al.*. 2004.

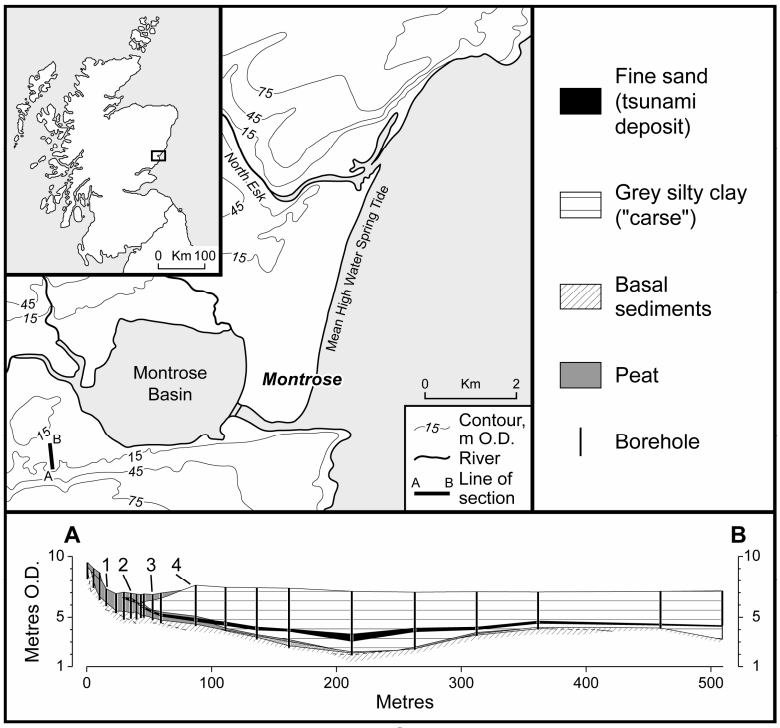

Fig. 4 The site at Fullerton, near Montrose, Scotland, showing the boreholes from which tsunami sand samples were taken. Based partly on Smith *et al.*. 2004.

beneath the surface of the peat. In recent work Moore *et al.* (in press) showed that the layer becomes thinner and fines landwards in general terms.

Monoliths from the peat containing the sand layer were taken at 5-10m intervals from the lagoon to the inland limit of the deposit (Figure 3). The location of each monolith was surveyed and its altitude levelled to local datum. On return to the laboratory, the sand layer at each monolith was sampled in contiguous 1cm slices and these samples analysed using a Malvern 2000 Mastersizer laser granulometer. Analyses involved pre-treatment using an acid digest to remove all organic matter, following the approach of Smith *et al.* (2004). The samples were obtained in August 1995 with the assistance of the Ottawa office of the Geological Survey of Canada and Erik Nielsen of Winnipeg, and analysed at Brighton University by Professor Callum Firth courtesy of Geomarine Associates Ltd.

Application of theory

The theoretical analysis can be applied to the twelve monolith samples taken along the shore-normal transect shown in Figure 3. The aim is to predict the water run-up distance from the observed sediment depositional characteristics. The SWL is taken as the shore of Taylor's Pond from extension of the line of section. The gradient of the land over this region increases landwards, with a mean gradient of about 1:22.

The Malvern granulometer gave results from each 1cm slice from each monolith as percentages of the total mass of sediment found in each of five grain-size fractions. The grain-size fractions with the largest masses of sediment were found to be those for 500-2000μm, 177-500μm, and 44-177μm, and these were chosen for the theoretical treatment. The percentages in all the slices for each monolith for a given grain-size fraction were summed, to give the percentage of sediment at that location attributable to that fraction. This was converted to give the contributions from each fraction to the thickness of deposit at that location. These are plotted for each of the three fractions and for the twelve locations in Figure 5a. Despite some scatter, due presumably to topographic features, it is seen that the thickness of each fractional deposit thins landwards. Linear trends have been fitted by least-squares regressions. From the trend-lines, the coarsest fraction (500-2000μm) has a thickness at the SWL of 3.4cm and a run-up distance of 115m. The corresponding figures for the medium fraction (177-500μm) are 4.1cm and 130m, and for the finest fraction (44-177μm) are 0.7cm and 166m. Thus, the run-up distances of the sediments (from the trend-lines) are greater for the finer sediments as predicted by the theory.

The settling velocities of the median diameters of each fraction (1000, 297, 88μm) are 0.114, 0.0368 and 0.00442 m/s for the coarse, medium and fine fractions respectively, using the formula of Soulsby (1997, Eq. 102) and assuming sea-water at 10°C and 35ppt with sediment density of 2650kg/m^3. Eq 7 can be applied to each fraction, yielding three equations in two unknowns, namely R_w and the quantity $B = \gamma T/H$ (with dimensions of inverse velocity), since the three values of R_s and w_s are known. A fitting procedure leads to an optimum value of B = 4.2s/m and R_w = 163m. The predicted run-up height is thus 163/22 = 7.4m above the local datum

(estimated tide level at the time of the tsunami). This compares with an observed run-up height from direct observations at the time of the tsunami of about 8.8m at this location (Tuttle *et al.* 2004) as seen in Figure 3.

APPLICATION 2: THE HOLOCENE STOREGGA SLIDE TSUNAMI

The Holocene Storegga Slide tsunami occurred around 8000 sidereal years BP. It is believed to have been generated by submarine sliding on the Continental Shelf and slope off South West Norway. The cause of the slide is unknown, but could have been due to crustal movement at the close of the last glaciation as Scandinavia became relieved of its ice burden (e.g. Smith *et al.* 2004).

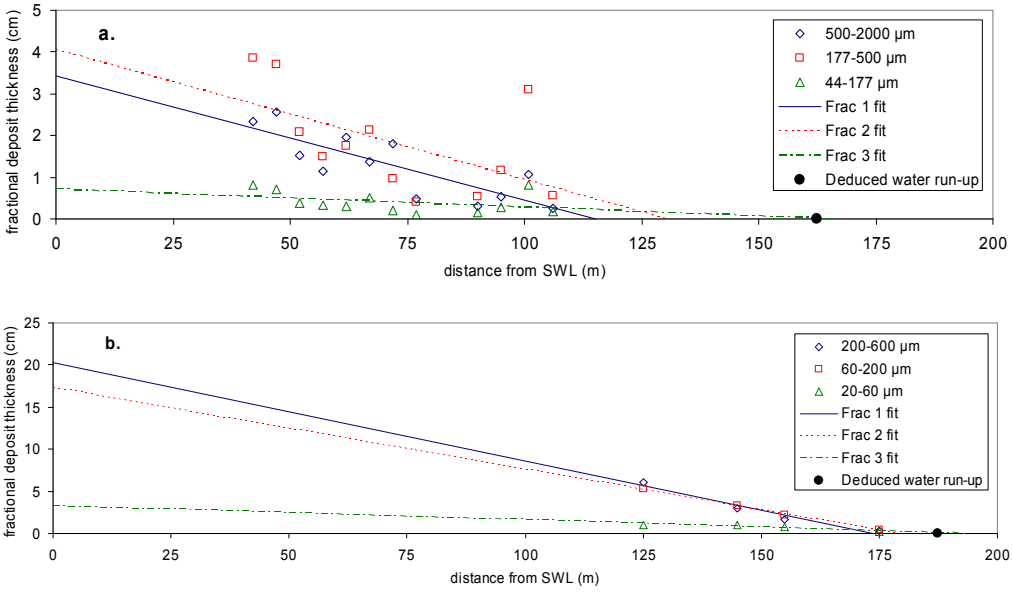

Fig. 5. Observed landwards variation of fractional deposit thickness, and fitted lines, for three grainsize fractions from (a) Taylor's Bay, Newfoundland, (b) Fullerton, Scotland.

The effect of the slide was to generate tsunami waves which inundated coastal areas as far apart as Iceland, the Faeroes, much of the Norwegian west coast, Scotland and northern England. At the time, sea surface levels lay up to 15m lower in the area (e.g. Mörner, 1980), but because of differential crustal depression following glaciation, relative sea levels across the coastlines involved were variable. The tsunami deposited in particular a distinctive layer of sand, normally less than 0.5m thick, across coastal peat, mudflat and saltmarsh. Subsequently, the layer was buried beneath later deposits of peat and coastal sediments. The layer is best preserved in former coastal inlets, usually gullies and small estuaries.

The sand layer at all sites was identified and sampled from shallow boreholes, using hand operated coring equipment. On return to the laboratory, contiguous 1cm samples were prepared for particle size analysis by removing all organic matter. Analysis was undertaken in a previous study by Shi (1995) using a Malvern 2600 laser granulometer as detailed by Smith *et al.* (2004).

The site used for this application is Fullerton (Figure 4), which lies at the western edge of the Montrose Basin, where a gully circa 1km long occurs in Late Glacial raised coastal terraces, to seaward of which raised Holocene estuarine sediments form an extensive surface. The tsunami sand layer can be traced along the gully and across its axis, and the sand has been analysed in four boreholes at the southern and of the transect. Two upward-fining sequences can be distinguished, but only the upper one is used in the present analysis as it is better defined. The site was described in Smith *et al.* (2004).

Application of theory

The theoretical analysis of the Fullerton section followed the same approach as for the Newfoundland example. Here, there were only four boreholes available. The origin of the x-coordinate (SWL) was taken at the lowest point on the section of the base of the sand layer, at about 210m on the section in Figure 4 where the elevation is 3.0mOD. The mean gradient of the land is about 1:30. The three grain-size fractions used in the analysis were 200-600μm, 60-200μm and 20-60μm. Roughly 10% of the sediments were finer than 20μm, but these were not used in the analysis. The thicknesses at the SWL, and the sediment run-up distances, taken from fitted lines (Figure 5b) for the coarse, medium and fine grain-size fractions were 20.3cm and 174m, 17.3cm and 179m, and 3.3cm and 194m respectively. The calculated settling velocities were 0.0447, 0.00682 and 0.000709m/s. The optimum values from the fitting procedure were B = 2.6s/m and R_w = 188m. The predicted run-up height is thus 188/30 = 6.3m above the assumed SWL, giving a total run-up height of 9.3mOD. In this case, there are no observations of water run-up, and the theory provides an estimate for an otherwise unknown quantity.

DISCUSSION

It is seen in both applications that the predicted run-up limit of the water is roughly equal to the projected limit of the finest sediment fraction. This is because the theory essentially equates the water run-up to the run-up of sediment with zero settling velocity, and the settling velocities of the finest sediments in both applications are very small. At Taylor's Bay, the observed water run-up height (about 8.8m) is rather larger than the predicted value (7.4m). This might be due to the simplifying assumption of no re-erosion of sediments in the theory, whereas in reality a thin layer of fine sediment deposited by the uprush could be eroded during the backwash.

Other departures of the idealised theory from the field situation include: (a) the actual topography is much more complex (gullies, ponds, ridges, vegetation) than the assumed smooth plane of constant slope, (b) laboratory experiments (O'Donoghue *et al.*, in press) show that the depth and velocity of a wave running up a sloping beach exhibit roughly parabolic and saw-tooth time-variations respectively, instead of the linear and constant time-variations respectively used in the simple theory, (c) the settling-column assumption for the sediments is an over-simplification. In practice, the sediment responds to a balance of erosion, deposition and diffusion processes.

In principle, a more sophisticated fitting technique between the theory and the data could be used. This could include the vertical grain-size variations, and might allow other tsunami characteristics such as wave height and period, water velocities, and suspended sediment concentrations to be deduced. However, the value of performing such a fitting would depend on how closely the idealisations of the theory conform to the geographical realities of individual sites.

The best way to overcome the deficiencies of the simple model would be to add sediment dynamics to a detailed numerical model of the tsunami hydrodynamics such as those of Borthwick *et al.* (2005) and O'Donoghue *et al.* (in press). This could model the two-dimensional flow patterns around complex topography, as well as the offshore sediment erosion, and the transport, deposition, re-erosion, convergence and divergence of sediment transport onshore. Optimisation of the input parameters such as height and period of the offshore wave could be performed to give a least-squares fit to the observed sediment thicknesses and grain-size compositions to achieve a full re-construction of depths, velocities and durations at all inundated points. More realistic tsunami inputs, such as multiple interacting waves, could also be modelled.

CONCLUSIONS

This analysis yields an equation for the maximum sediment run-up distance (R_s) in terms of the water run-up distance (R_w), and two additional parameters $\alpha = \frac{w_s T}{H}$, and γ = ratio (duration of uprush)/(duration of backwash) at the SWL. Here H is the height of the tsunami wave, and T the duration of inundation, at the SWL. A second equation gives the maximum deposit thickness (at the SWL) ζ_o in terms of α, γ, H, C_0 and the bulk density of the deposited sediment. The derived variation in thickness of the sediment deposit is found to decrease linearly with landward distance, from ζ_o at the SWL to zero at distance R_s. Applying the model with a range of grainsizes yields the following features, which agree with observations:

- The thickness of the deposit decreases uniformly with distance from the SWL
- The limit of the sediment deposit falls well short of the water run-up limit
- The landward extent of the sediment deposit increases with decreasing grain-size, so that the net result is a landward fining of the sediment
- Very coarse sediments are all deposited close to the SWL.
- Very fine sediments are almost entirely swept back out to sea
- Because of differential settling velocities, an upward fining sequence is formed
- Successive tsunami waves can give rise to multiple upward fining sequences

The theory has been applied to sediment samples from Newfoundland deposited by the 1929 "Grand Banks" tsunami, where the water run-up distance and height are known from observations at the time. Reasonably good agreement between predicted and observed run-up were found. The method has also been applied to sediment deposits in Scotland resulting from the Holocene Storegga Slide tsunami to deduce the water run-up distance and height, which in this case are not known. Thus

here the new method allows additional information to be deduced from the sediment deposits.

REFERENCES

Borthwick, A. G. L., Ford, M., Taylor, P. H., Weston, B. P. and Stansby, P.K. (2005). "Prediction of solitary wave run-up at an arbitrary plane beach," *Waves 2005, Conference Proc.*, *on CD-ROM, IAHR*, Paper No. 101, 9p.

Dawson, A. G. and Shi, S. (2000). "Tsunami deposits," *Pure and Applied Geophysics* 157, 875-897.

Jaffe, B. and Gelfenbaum, G. (2002). "Using tsunami deposits to improve assessment of tsunami risk," *Solutions to Coastal Disasters '02, Conference Proc., ASCE*, 836-847.

Jaffe, B. and Gelfenbaum, G. (in press). "A simple model for calculating tsunami flow speed from tsunami deposits," *Special Issue on Tsunami Deposits, Sedimentary Geology*.

Matsutomi, H., Shuto, N., Imamura, F. and Takahashi, T. (2001). "Field survey of the 1996 Irian Jaya Earthquake Tsunami in Biak Island," *Natural Hazards* 24, 199-212.

Moore, A. L. (2001). "Grain-size trends in a Holocene tsunami deposit from Cultus Bay, Puget Sound, Washington," *International Tsunami Society Proceedings*, Session 3(3-6), 503-510.

Moore, A., McAdoo, B. and Ruffman, A. (in press). "Landward fining from multiple sources in a sand sheet deposited by the 1929 Grand Banks tsunami, Newfoundland," *Special Issue on Tsunami Deposits, Sedimentary Geology*.

Mörner, N. A. (1980). "Late Quaternary sea-level changes in north-west Europe: a synthesis," *Geologiska Foreningens i Stockholm Forhandlingar* 100, 381-400.

O'Donoghue, T., Hondebrink, L. and Pokrajac, D. (in press). "Bore-driven swash on beaches: numerical modelling and large-scale laboratory experiments," *Proc. 30th International Conference on Coastal Engineering, World Scientific Publishing*.

Ruffman, A. and Hann, V. (2006). "The Newfoundland Tsunami of November 18, 1929: An Examination of the Twenty-eight Deaths of the "South Coast Disaster,"" *Newfoundland and Labrador Studies* 21(1), 97-148.

Shi, S. (1995). "Observational and theoretical aspects of Tsunami sedimentation," Unpublished PhD thesis, Coventry University.

Smith, D. E., Shi, S., Cullingford, R. A., Dawson, A. G., Dawson, S., Firth, C. R., Foster, I. D. L., Fretwell, P. T., Haggart, B. A., Holloway, L. K. and Long, D. (2004). "The Holocene Storegga Slide tsunami in the United Kingdom," *Quaternary Science Reviews* 23, 2291-2321.

Smith, D. E., Foster, I. D. L., Long, D. and Shi, S. (in press). "Reconstructing the pattern and depth of flow onshore in a palaeotsunami from associated deposits", *Special Issue on Tsunami Deposits, Sedimentary Geology*.

Soulsby, R. L. 1997. "*Dynamics of Marine Sands*", Thomas Telford, London, 249 p.

Tuttle, M. P., Ruffman, A., Anderson, T. and Jetter, H. (2004). "Distinguishing tsunami from storm surge deposits in eastern North America: the 1929 Grand Banks tsunami versus the 1991 Halloween storm," *Seismological Research Letters* 75(1), 117-131.